Edelweiss Applied Science and Technology
ISSN: 2576-8484
Vol. 9, No. 6, 1905-1917
2025
Publisher: Learning Gate
DOI: 10.55214/25768484.v9i6.8276

Numerical and experimental study of primary drying stage in freeze-drying of Cordyceps militaris

Phuc V Nguyen[1,2*], An N Nguyen[1]
[1]Faculty of Thermal Energy, School of Mechanical Engineering, Ha Noi University of Science and Technology, Ha Noi, Viet Nam; an.nguyennguyen@hust.edu.vn (A.N.N.).
[2]Faculty of Mechanical Engineering, Nha Trang University, Khanh Hoa, Viet Nam; phucnv@ntu.edu.vn (P.V.N.).

Abstract: This study develops a mathematical model to simulate the heat and mass transfer processes during the freeze-drying of cylindrical biological materials, with Cordyceps militaris fibers serving as the representative case. The model accounts for the coupled mechanisms of heat conduction and vapor diffusion within the porous structure. A one-dimensional system of partial differential equations is established and solved using the finite difference method implemented in MATLAB. The simulation outputs include the temporal evolution of surface temperature, dry region temperature, moisture content, internal energy, and the position of the sublimation front. Model validation was conducted through experimental comparison, yielding average percentage errors of 0.98% for temperature, 7.12% for moisture ratio, and 6.24% for drying time, resulting in an overall error of 5.5%. These results confirm the model's reliability in capturing key drying dynamics. The study concludes that accurate modeling of coupled heat and mass transfer is essential for predicting freeze-drying behavior. The findings offer a theoretical foundation for optimizing freeze-drying protocols for Cordyceps militaris and similar cylindrical structures, contributing to improved energy efficiency and product quality in practical applications.

Keywords: *Freeze-drying, Heat and mass transfer, Cordyceps militaris.*

1. Introduction

Freeze-drying, also known as lyophilization, is a drying method with significant advantages, particularly in preserving product quality. Products dried by this method retain most of their nutrients and valuable bioactive compounds, with minimal changes in shape and color [1-6]. However, freeze-drying is a complex and high-cost process, heavily influenced by factors such as drying regimes, technological procedures, and material properties [7, 8]. To reduce production costs and improve product quality, studies on heat and mass transfer during freeze-drying have become a key focus in scientific research. Modeling and optimizing the freeze-drying process have been applied to enhance efficiency and product quality for various materials.

The freeze-drying process of food usually consists of three main stages. The first stage is the freezing stage, in which the moisture in the material is completely frozen, preparing it for the subsequent sublimation process. This is followed by the primary drying stage (also known as sublimation), which is the most important and time-consuming stage, greatly affecting the quality of the product. During this stage, the ice in the frozen material is removed through the sublimation process. Finally, the secondary drying stage (desorption) is performed at a higher temperature to remove the remaining moisture, mainly in the form of bound water that did not freeze in the initial stage. If the material's moisture is entirely frozen during the freezing stage or if the required moisture level is achieved after the primary drying stage, the secondary drying stage can be omitted [9].

History: Received: 23 April 2025; Revised: 2 June 2025; Accepted: 6 June 2025; Published: 21 June 2025
* Correspondence: phucnv@ntu.edu.vn

During freeze-drying, a dynamic sublimation front is formed, dividing the material into two regions: the dried and the frozen regions. With a well-designed drying process and parameters, the dried product retains its original size and shape, and its porosity significantly increases. Consequently, the dried material in the dry region exhibits characteristics similar to porous materials. The sublimation process is influenced by heat transfer and moisture diffusion through the porous region [10, 11].

Several authors, including Jafar and Farid [12]; von Graberg [13]; Varma [14]; Trelea, et al. [15]; Scutellà, et al. [16] and Gustafsson [17] have assumed the heat and mass transfer processes during freeze-drying as "quasi-steady". These studies typically employed the Fourier's law of heat conduction, the Stefan-Boltzmann law of thermal radiation, energy balance equations, and mass balance equations to develop mathematical models describing the heat and mass transfer phenomena in drying materials.

Numerous studies have developed mathematical models to describe the freeze-drying process for materials with various shapes, such as flat (sheet) or spherical (bead) forms. However, there has been limited research on cylindrical-shaped materials. This study focuses on developing a mathematical model to describe the heat and mass transfer processes of cylindrical materials during freeze-drying, with *Cordyceps militaris* (*Cordyceps militaris*) fibers as a representative case.

2. Materials and Methods

2.1. Materials

The study material is the fruiting body of *Cordyceps militaris*, an artificially cultivated fungus used as a functional food for the prevention and treatment of various fatal diseases. It is highly valued for its rich content of vitamins, amino acids such as adenosine, cordycepin, and other rare bioactive components [18, 19]. *Cordyceps militaris* is a fungus belonging to the family Cordycipitaceae and is the representative species of the genus Cordyceps [19]. Its fruiting body is cylindrical, orange in color, with a length of 5 to 8 cm and a diameter of 3 to 6 mm.

2.2. Model structure

Cordyceps militaris fibers are cylindrical in shape, with a radius r_s, (m) and a length L_s, (m). They are arranged in a single layer within a drying tray placed inside the drying chamber. A heating rack is attached to the bottom of the tray, allowing the temperatures of both the tray and the rack to be considered equal. A vapor condenser plate is mounted above the tray, inside the drying chamber, as illustrated in Figure 1.

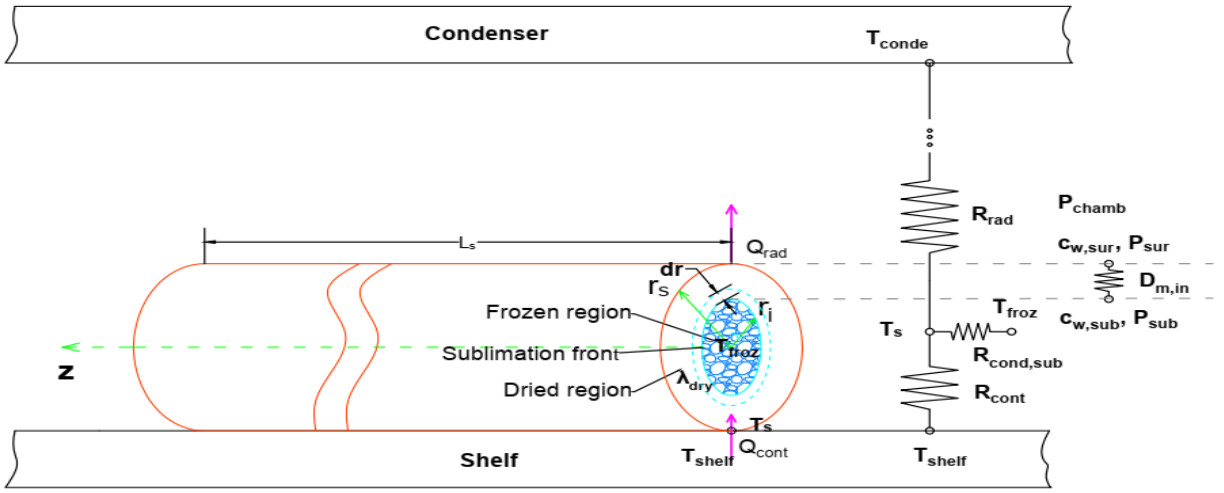

Figure 1.
Schematic diagram heat transfer and mass transfer of *Cordyceps militaris* in the drying tray.

Edelweiss Applied Science and Technology
ISSN: 2576-8484
Vol. 9, No. 6: 1905-1917, 2025
DOI: 10.55214/25768484.v9i6.8276

2.3. Initial Assumptions

These assumptions have also been adopted in several previous studies that developed mathematical models for heat and mass transfer in the freeze-drying process [12, 14-16, 20-23].

- The heat and mass transfer process occurs uniformly across all *Cordyceps militaris* fibers. In each fiber, ice sublimates at a distinct sublimation front, which separates two coaxial cylindrical regions: a dry outer region and a frozen inner core. As drying proceeds, the dry region expands while the frozen region shrinks. The primary drying phase is considered complete when the frozen region vanishes.
- Throughout drying, the frozen region maintains constant temperature and moisture content, with its temperature equal to that at the sublimation interface ($T_{froz} = T_{sub} = const$).
- Assuming that the *Cordyceps militaris* fiber's length is much larger than its diameter, axial heat and mass transfer is negligible. The fiber can therefore be approximated as an infinitely long cylinder.
- Heat supplied from the drying tray is partly used for sublimation in the frozen region and partly increases the temperature of the dry region, with the remainder transferred to the vapor condenser. Radiative heat exchange with chamber walls is neglected.
- Based on these assumptions, the heat and mass transfer model is developed in a radially symmetric cylindrical coordinate system with a single spatial variable r.

2.4. The Heat and Mass Transfer Equation

Based on the heat and mass transfer diagram (Figure 1) and the initial assumptions, a mathematical model can be developed to describe the drying process of *Cordyceps militaris* fiber using the sublimation method.

2.4.1. Heat Transfer Equations in the Freeze-Drying Process of Cordyceps Militaris

Energy balance equation for *Cordyceps militaris* fiber:

$$Q_{cont} = Q_u + Q_{sub} + Q_{rad} \tag{1}$$

Where Q_{cont} is heat transferred from the drying tray to the *Cordyceps militaris* fiber, defined by:

$$Q_{cont} = \frac{T_{shelf} - T_s}{R_{cont}} \tag{2}$$

With R_{cont} is heat transfer resistance due to contact:

$$R_{cont} = \left(\frac{1}{R_{cond,tr}} + \frac{1}{R_{rad,tr}} \right)^{-1} \tag{3}$$

Heat required to change the temperature of the dried region Q_u calculated as [24]:

$$Q_u = \frac{dU_{dry}}{d\tau} \tag{4}$$

The internal energy of the dry region in the *Cordyceps militaris* fiber is determined by the following equation [25]:

$$U_{dry} = \int_{r_{bth}}^{r_s} C_{dry} \cdot T_{dry} \cdot \rho_{dry} \cdot 2\pi \cdot r \cdot L_s \cdot dr \tag{5}$$

The temperature distribution in the dried region of the *Cordyceps militaris* fiber is assumed to follow quasi-steady radial heat conduction in a cylindrical geometry, neglecting axial conduction. Accordingly, the temperature at a radial position r can be calculated by the following logarithmic expression [24]:

Edelweiss Applied Science and Technology
ISSN: 2576-8484
Vol. 9, No. 6: 1905-1917, 2025
DOI: 10.55214/25768484.v9i6.8276

$$T_{dry} = T_{sub} + \frac{Q}{2\pi \cdot k_{dry} \cdot L_s} \cdot \ln\left(\frac{r}{r_{sub}}\right) \quad (6)$$

Considering the surface of the fiber, we have: r = r_s and T_{dry} = T_s. In this case, Equation (6) becomes:

$$\frac{Q}{2\pi \cdot k_{dry} \cdot L_s} = \frac{T_{sub} - T_s}{\ln\left(\frac{r_s}{r_{sub}}\right)} \quad (7)$$

Substituting Equation (7) into Equation (6), we obtain:

$$T_{dry} = T_{sub} + \frac{T_s - T_{sub}}{\ln\left(\frac{r_s}{r_{sub}}\right)} \cdot \ln\left(\frac{r}{r_{sub}}\right) \quad (8)$$

Heat supplied for sublimating ice at the sublimation front Q_{sub} defined by:

$$Q_{sub} = \frac{T_s - T_{sub}}{R_{cond,sub}} \quad (9)$$

Heat transfer resistance between the surface of the fiber and sublimation front $R_{cond,sub}$ calculated as [24]:

$$R_{cond,sub} = \frac{\ln\left(\frac{r_s}{r_{sub}}\right)}{2\pi \cdot k_{dry} \cdot L_s} \quad (10)$$

The heat Q_{sub} is also the energy required for sublimation, and the sublimation rate is given by:

$$\dot{G} = \frac{Q_{sub}}{L_{sub}} = \frac{T_s - T_{sub}}{R_{cond,sub} \cdot L_{sub}} \quad (11)$$

Heat radiated by the fiber to the vapor condenser plate Q_{rad} defined by:

$$Q_{rad} = \frac{T_s - T_{conde}}{R_{rad}} \quad (12)$$

2.4.2. Moisture Transfer Equation in the Freeze-Drying Process of Cordyceps Militaris:

The sublimation rate of the ice in the *Cordyceps militaris* fiber corresponds to the vapor diffusion rate from the sublimation interface to the fiber surface through the dried region, determined by Fick's first law [24]:

$$J_w = -D_{eff} \cdot \frac{dc_w}{dr} \quad (13)$$

The mass of water vapor moving from the sublimation interface through the dry region to the outside of the fiber is:

$$\dot{G} = A_{sub} \cdot J_w = -\left(2.\pi.L_s.r\right).D_{eff} \cdot \frac{dc_w}{dr} \quad (14)$$

Where, cw is moisture vapor concentration, [kg/m³]

Edelweiss Applied Science and Technology
ISSN: 2576-8484
Vol. 9, No. 6: 1905-1917, 2025
DOI: 10.55214/25768484.v9i6.8276

$$c_w = \frac{P_w \cdot M_w}{R_g \cdot T} \tag{15}$$

Mass balance equation at the sublimation interface:

The position of the moving sublimation interface is determined based on the mass balance equation. Assuming that moisture in the freeze-dried material is uniformly distributed throughout the fiber volume, the radial position of the sublimation interface is determined from the relationship [15]:

$$\frac{dr_{sub}}{d\tau} = -\frac{\dot{G}}{A_{sub}.\rho_{ice,eff}} = -\frac{\dot{G}}{(2.\pi.L_s.r_{sub}).\rho_{ice,eff}} \tag{16}$$

2.5. Numerical Method for Solving the Heat and Mass Transfer Mathematical Model

To solve the mathematical model simulating the the heat and mass transfer during the freeze-drying process of *Cordyceps militaris*, this study employs the finite difference method with the support of MATLAB 2021b software.

2.6. The experimental freeze-drying

Freeze-drying experiments for Cordyceps were performed on a freeze dryer at the laboratory of Nha Trang University, equipment details are shown in Figure 2.

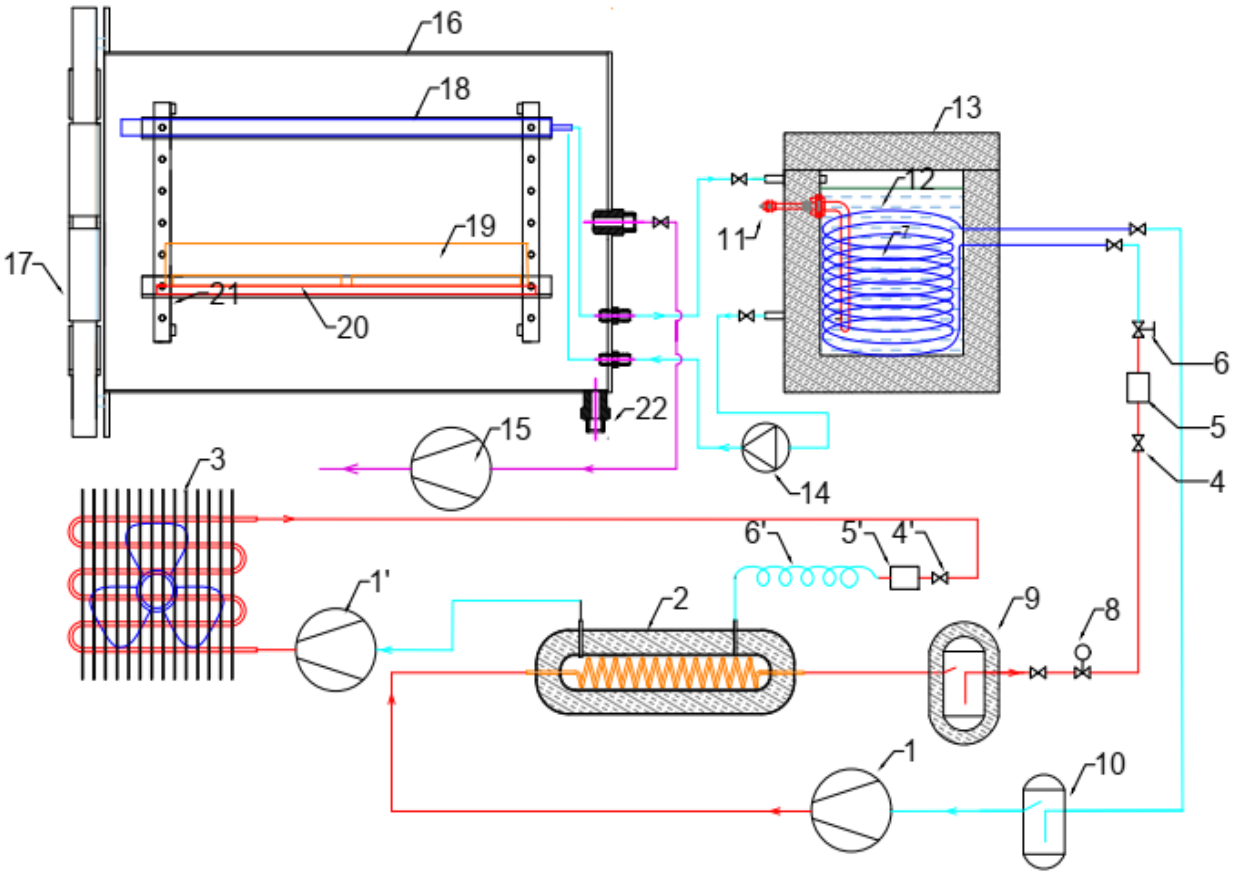

Figure 2.
Schematic diagram of the freeze dryer used in the experiment.

Edelweiss Applied Science and Technology
ISSN: 2576-8484
Vol. 9, No. 6: 1905-1917, 2025
DOI: 10.55214/25768484.v9i6.8276

1. Compressor; 2. Cascade heat exchanger; 3. Condenser unit; 4. Valve; 5. Filter; 6. Expansion valve; Evaporator unit; 8. Solenoid valve; 9. High pressure tank; 10. Liquid separator; 11. Heater; 12. Coolant; 13. Coolant tank; 14. Pump; 15. Vacuum pump; 16. Drying chamber; 17. Door; 18. Condenser plate; 19. Dryer tray; 20. Heating shelf; 21. Shelf frame; 22. Drain valve

The equipment includes: a 0.4 m^3 cylindrical sublimation chamber, a cascade refrigeration system to ensure the temperature of the vapor condenser plate is maintained at -35°C, a resistance heating plate is attached to the drying tray, a 2-stage oil ring vacuum pump can ensure the pressure in the sublimation chamber reaches 20 Pa... In addition, the temperature and pressure in the sublimation chamber are monitored, the temperature of the heating shelf is controlled by the PID method to ensure stable maintenance of the drying mode parameters, sensors to monitor the temperature of the drying material are installed in the drying chamber.

A temperature-measuring device with 12 measuring channels (Data logger Extech TM500, Extech Instruments, Boston, Massachusetts, USA) was used. The temperature probe is inserted into the surface of *Cordyceps militaris* fibers. The temperature value of the fiber will be stored in the memory by the measuring device during the drying process.

The study used a pressure measuring device with model: Testo 552, measuring range: 0 to 2000 Pa to measure the pressure in the drying chamber. A stop valve was installed on the suction line of the vacuum pump to control the pressure in the drying chamber.

The equipment used in the study to weigh and measure the moisture content of material was Ohaus MB120 (readability: 0.01% or 0.001 g).

2.7. Method For Calculating the Error Between Simulation and Experimental Data

Method for calculating the Error between simulation and experimental data:

To evaluate the deviation between simulated and experimental values, the mean percentage error (*E*r %) can be used [25, 26].

$$\mathrm{Er}_i = \frac{100}{n}\sum \frac{\left|Y_{i,sim} - Y_{i,ex}\right|}{Y_{i,sim}} \tag{17}$$

The total average percentage error, considering the temperature, moisture ratio, and time, is calculated as follows:

$$\mathrm{Er}_{tol} = \sqrt{\frac{\left(\mathrm{Er}_T^2 + \mathrm{Er}_{MR}^2 + \mathrm{Er}_\tau^2\right)}{3}} \tag{18}$$

3. Results

Based on the heat and mass transfer equations, together with the initial conditions, thermophysical properties, and other characteristic parameters listed in Table 1, the mathematical model was solved using MATLAB. The results are presented in detail in the following sections.

Edelweiss Applied Science and Technology
ISSN: 2576-8484
Vol. 9, No. 6: 1905-1917, 2025
DOI: 10.55214/25768484.v9i6.8276

Table 1.
Physical properties and parameters used for simulation.

No	Symbol	Units	Value
1	r_s	m	0.00259
2	L_s	m	0.079
3	MR_0	kg/kgDb	3.762
4	M_w	kg/kmol	18
5	R_g	J/(kmol·K)	8314
6	L_{sub}	J/kg	3195667
7	T_{froze}	K	242.6
8	T_{sub}	K	242.6
9	T_{shelf}	K	273.2
10	T_{conde}	K	241.2
11	P_{chamb}	Pa	35
12	ρ_{dry}	kg/m³	277.08
13	$\rho_{ice,eff}$	kg/m³	832.22
14	C_{dry}	J/(kg·K)	1850
15	D_{eff}	m²/s	$4.52 \cdot 10^{-3}$
16	R_{rad}	K/W	3400.75
17	R_{cont}	K/W	78.5

3.1. Temperature and Moisture Distribution During the Freeze - Drying Process

The results of solving the heat and mass transfer mathematical model using MATLAB are presented in Figure 2 and Figure 3. These simulation results indicate that the primary drying stage ends after 15060 seconds from the start of drying. At this time, the average temperature of the dry region rises rapidly, approaching the surface temperature of the fiber at 262.9 K. The sublimation front has reached the center (r_{sub} = 0 m), and the product moisture content is 0.074 kg/kg dry basis, corresponding to 7% on a wet basis.

At the initial stage of drying, when the dry region on the outside of the fiber is newly formed and still thin, the mass transfer resistance is low, leading to a high sublimation rate. After approximately 8000 seconds, the dry region of the *Cordyceps militaris* fiber thickens, increasing the mass transfer resistance, which significantly reduces the sublimation rate.

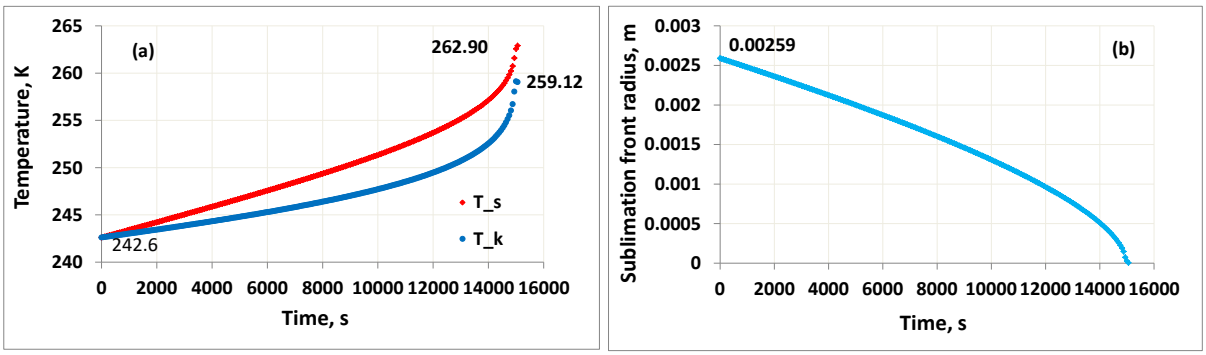

Figure 3.
a) Changes in the average temperature of the dry region and the surface of the *Cordyceps militaris* strand. b) Changes in the sublimation boundary radius of the *Cordyceps militaris* strand over drying time.

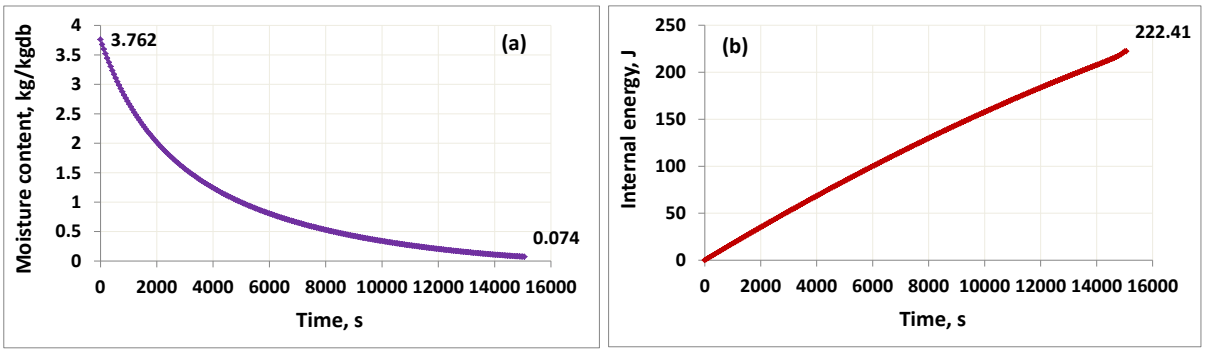

Figure 4.
Changes in the dry-basis moisture content (a) and internal energy of the *Cordyceps militaris* during drying time.

The simulation results show that the surface temperature of the fiber is consistently higher than the average temperature of the dry region. Near the end of the sublimation drying stage, the average temperature of the dry region rises rapidly, approaching the surface temperature of the fiber. Around 14000 seconds after the drying process starts, the temperature of the fiber rises quickly, approaching the shelf temperature. Along with that, the internal energy of the dry region increases faster. At this point, most of the moisture in the *Cordyceps militaris* fiber has sublimated, leaving only a small amount of residual moisture. This results in a reduced sublimation rate, and the heat supplied by the shelf mainly increases the temperature of the fiber.

3.2. Temperature and moisture distribution during the freeze - drying process

The simulation results show that the temperature in the dry region changes over both time and position. As drying progresses, the temperature of the dry region increases. Radially, the outer region exhibit higher temperatures than the inner ones. However, the rate of temperature increase is not uniform; it accelerates during the later stages of the drying process.

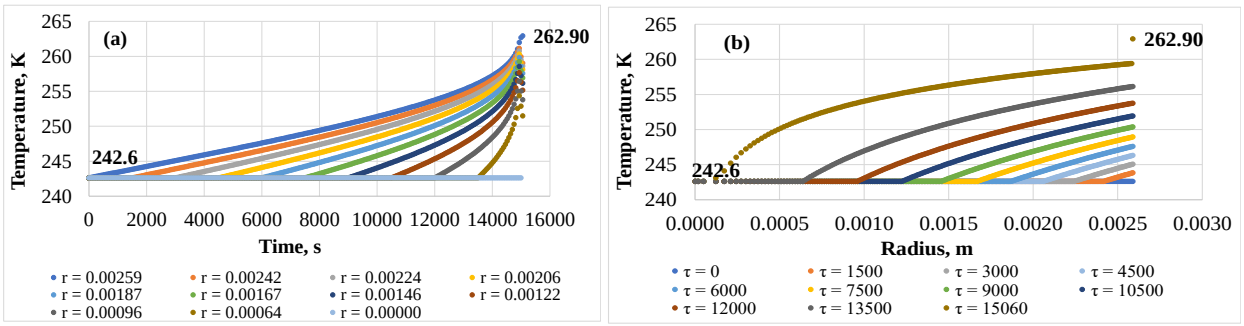

Figure 5.
Temperature variation in the dried region of *Cordyceps militaris*: (a) over time at different radius; (b) along radius at different times.

Notably, in the final phase of sublimation, the temperature in the dry region rises sharply. This behavior is attributed to the increasing thermal resistance caused by the thickening of the dry region. Once sublimation ends due to the depletion of residual moisture, the supplied heat primarily contributes to a rapid temperature rise in the dry region, eventually approaching the surface temperature of the *Cordyceps militaris* fiber.

Edelweiss Applied Science and Technology
ISSN: 2576-8484
Vol. 9, No. 6: 1905-1917, 2025
DOI: 10.55214/25768484.v9i6.8276

3.3. The Sublimation Rate

The calculated results for the sublimation rate and the proportion of sublimated moisture over time are shown in Figure 6(a). It can be observed that the sublimation rate gradually decreases throughout the drying period. Initially, it reaches a maximum value of 1.2×10^{-7} kg/s, but then declines significantly toward the end of the process, dropping to approximately 3.6×10^{-8} kg/s.

Furthermore, as the drying process progresses, the temperature of the dry region rises, which increases the vapor pressure within the dry region. This reduces the pressure difference between the sublimation front and the dry region, thereby decreasing the driving force for vapor diffusion through the dry region to the surface of the *Cordyceps militaris* fiber. Figure 6(b) illustrates that during the initial 9000 seconds, the majority of the moisture in the *Cordyceps militaris* (approximately 90 %) is sublimated. Over the remaining period from 9000 to 15060 seconds, only about 8 % of the moisture undergoes sublimation.

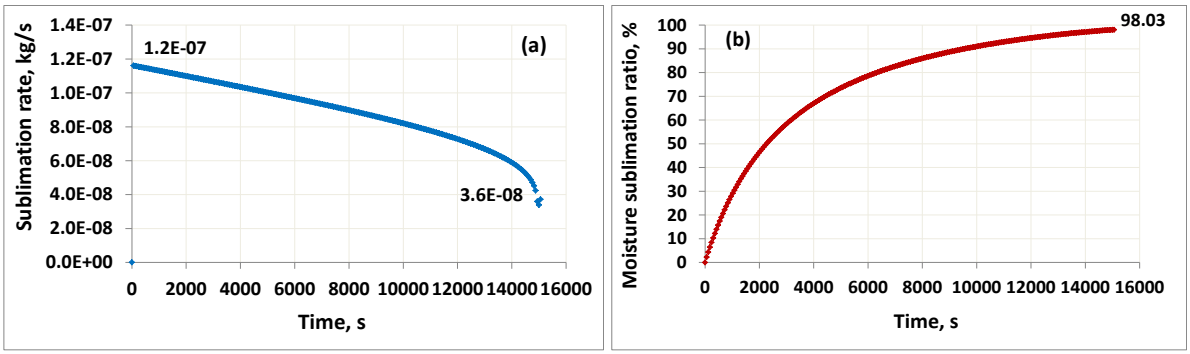

Figure 6.
The sublimation rate and the fraction of sublimated moisture over time.

The results of the study on the variation of residual vapor concentration in the dry region of *Cordyceps militaris* fibers over position and time are presented in Figure 7. After sublimation occurs at the moving sublimation front, part of the generated vapor diffuses to the fiber surface and escapes from the drying chamber, while the remainder accumulates within the dry region. The amount of residual moisture in the dry region decreases over time and shows a decreasing gradient from the sublimation front toward the fiber surface. The inner dry region near the core exhibit higher vapor concentrations compared to the outer layers and the surface. This phenomenon is attributed to the increasing mass transfer resistance in the dry region as the distance from the sublimation front to the fiber surface increases. The variation in vapor concentration affects the thermal conductivity of the dry region, which in turn influences the moisture sublimation rate during the drying process.

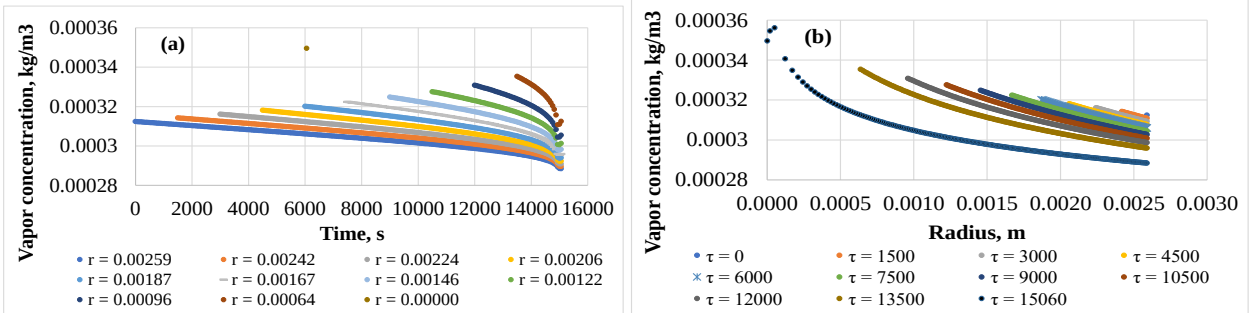

Figure 7.
Distribution of residual vapor concentration in the dried region of *Cordyceps militaris*: (a) over time at different radii; (b) along radius at different times.

Edelweiss Applied Science and Technology
ISSN: 2576-8484
Vol. 9, No. 6: 1905-1917, 2025
DOI: 10.55214/25768484.v9i6.8276

3.4. Comparison of Simulation and Experimental Results

The study conducted an experimental freeze-drying process of *Cordyceps militaris* under the following conditions: heating plate temperature T_{shelf} = 273.2 K, condensing plate temperature T_{conde} = 241.2 K, and drying chamber pressure P_{champ} = 35 Pa. The comparison between the surface temperature and moisture content of *Cordyceps militaris* obtained from simulation and experiment is illustrated in Figure 8.

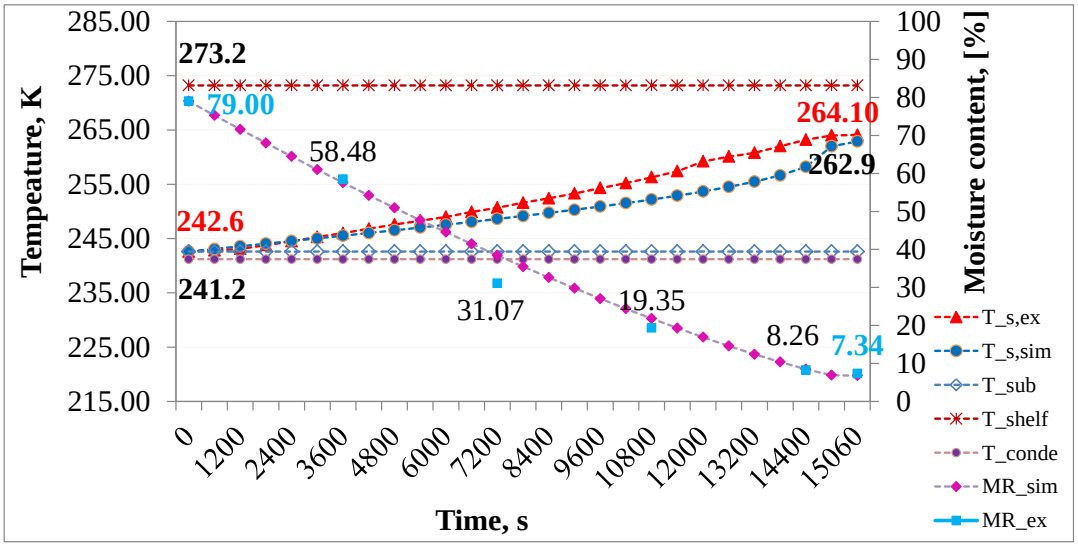

Figure 8.
Comparison of simulated and experimental results in the freeze-drying of *Cordyceps militaris*.

The results indicate a good agreement between simulated and experimental data. In terms of trends, during the initial two-thirds of the drying period, the temperature rose gradually, while the drying rate was relatively higher. Conversely, in the later stage, the temperature increased more rapidly, approaching the heating plate temperature, whereas the drying rate slowed down. Toward the end of the freeze-drying phase, the moisture content decreased steadily to approximately 7% (wet basis).

Overall, the experimental temperatures were generally higher than the simulated values, especially during the final phase of drying. This discrepancy may be attributed to changes in the thermophysical properties and internal structure of the *Cordyceps militaris* fiber, which can influence the actual heat and mass transfer behavior.

The average percentage errors between simulation and experiment were calculated as follows: temperature error E_T = 0.98 %, moisture ratio error E_{MR} = 7.12 %, and time error E_τ = 6.24 %. The total average percentage error considering all three factors was Er_{tol} = 5.5 %. Heldman and Lund [27] suggested that mathematical models describing the kinetics of drying processes may allow errors of up to 12%. These results indicate that the developed mathematical model, along with the applied boundary conditions and material properties, is appropriate for describing the heat and mass transfer processes involved in the freeze-drying of *Cordyceps militaris*.

Thus, to achieve a final moisture content of 7% at a sublimation chamber temperature of 273.2 K, the required drying time is approximately 15060 s. In the study by Wu, et al. [2] the freeze-drying process of *Cordyceps militaris* from an initial moisture content of 80% to 5% was conducted at chamber temperatures ranging from 40 °C to 70 °C, with the pressure maintained at 80 Pa. The total drying time varied from 6 h to 9.3 h depending on the temperature conditions, during which the sublimation stage lasted from 3 h to 5.83 h. A comparison shows that at higher temperature settings, the drying times reported by Xiao–Fei Wu et al. were shorter than those in this study; conversely, under lower

Edelweiss Applied Science and Technology
ISSN: 2576-8484
Vol. 9, No. 6: 1905-1917, 2025
DOI: 10.55214/25768484.v9i6.8276

temperature conditions, the drying times were longer. This discrepancy is primarily attributed to differences in the drying parameters. Although the present study employed lower drying temperatures, the sublimation chamber pressure was kept lower, thereby maintaining an adequate sublimation rate. Nevertheless, increasing the drying temperature could further enhance the drying rate, but it may also pose risks such as structural collapse, increased shrinkage, and deterioration of product quality.

4. Conclusion

Thus, the mathematical model describing the heat and mass transfer processes has been established, clearly illustrating the mutual coupling between heat and mass transfer during the freeze-drying of cylindrical *Cordyceps militaris* fibers. Specifically, the sublimation rate depends on the heat flux from the fiber surface to the sublimation front, which in turn is influenced by the thermal conductivity and thickness of the dry region. Conversely, the thermal conductivity of the dry region is affected by the vapor concentration within it, which is governed by the sublimation rate and the mass transfer resistance of the dry region. This reciprocal relationship is a key factor incorporated into the model to ensure that the simulation accurately captures the physical behavior of the freeze-drying process.

The results obtained from solving the heat and mass transfer equations revealed the temperature field at the surface and within the dry region, the moisture content distribution, the internal energy of the dry region, and the position of the sublimation front in *Cordyceps militaris* fiber. These results also demonstrated the influence of both thermal resistance and mass transfer resistance on the heat and mass transfer processes, particularly highlighting the sharp increase in material temperature during the final stage of drying. This serves as an important basis for selecting appropriate drying conditions to ensure product quality while minimizing drying time.

Transparency:

The authors confirm that the manuscript is an honest, accurate, and transparent account of the study; that no vital features of the study have been omitted; and that any discrepancies from the study as planned have been explained. This study followed all ethical practices during writing.

References

[1] X.-F. Wu, M. Zhang, and Z. Li, "Influence of infrared drying on the drying kinetics, bioactive compounds and flavor of Cordyceps militaris," *LWT*, vol. 111, pp. 790-798, 2019. https://doi.org/10.1016/j.lwt.2019.05.108

[2] X.-F. Wu, M. Zhang, and B. Bhandari, "A novel infrared freeze drying (IRFD) technology to lower the energy consumption and keep the quality of Cordyceps militaris," *Innovative Food Science & Emerging Technologies*, vol. 54, pp. 34-42, 2019. https://doi.org/10.1016/j.ifset.2019.03.003

[3] T. Chimsook, "Effect of freeze drying and hot air drying methods on quality of cordycepin production," presented at the MATEC Web of Conferences, 2018.

[4] Y. Li, H. Yang, H. Yang, J. Wang, and H. Chen, "Assessment of drying methods on the physiochemical property and antioxidant activity of Cordyceps militaris," *Journal of Food Measurement and Characterization*, vol. 13, pp. 513-520, 2019. https://doi.org/10.1007/s11694-018-9965-3

[5] X. f. Wu, M. Zhang, B. Bhandari, and Z. Li, "Effects of microwave-assisted pulse-spouted bed freeze-drying (MPSFD) on volatile compounds and structural aspects of Cordyceps militaris," *Journal of the Science of Food and Agriculture*, vol. 98, no. 12, pp. 4634-4643, 2018. https://doi.org/10.1002/jsfa.8993

[6] M. Heydari, K. Khalili, and Y. Ahmadi, "Simulation of stresses induced by heat and mass transfer in drying process of clay-like material," *Journal of Computational Applied Mechanics*, vol. 48, no. 2, pp. 171-184, 2017.

[7] D. Nowak and E. Jakubczyk, "The freeze-drying of foods—The characteristic of the process course and the effect of its parameters on the physical properties of food materials," *Foods*, vol. 9, no. 10, p. 1488, 2020. https://doi.org/10.3390/foods9101488

[8] J. Welti, F. Vergara, E. Pérez, and A. Reyes, "Fundamentals and new tendencies of freeze-drying of foods. University of the Americas," presented at the Second International Symposium on Food Innovation and Development, 2005.
[9] G. Nireesha, L. Divya, C. Sowmya, N. Venkateshan, and V. Lavakumar, "Lyophilization/freeze drying-an review," *International Journal of Novel Trends in Pharmaceutical Sciences*, vol. 3, no. 4, pp. 87-98, 2013.
[10] P. Levin, M. Buchholz, V. Meunier, U. Kessler, S. Palzer, and S. Heinrich, "Comparison of Knudsen diffusion and the dusty gas approach for the modeling of the freeze-drying process of bulk food products," *Processes*, vol. 10, no. 3, p. 548, 2022. https://doi.org/10.3390/pr10030548
[11] M. Krokida, V. Karathanos, and Z. Maroulis, "Effect of freeze-drying conditions on shrinkage and porosity of dehydrated agricultural products," *Journal of Food Engineering*, vol. 35, no. 4, pp. 369-380, 1998. https://doi.org/10.1016/S0260-8774(98)00031-4
[12] F. Jafar and M. Farid, "Analysis of heat and mass transfer in freeze drying," *Drying Technology*, vol. 21, no. 2, pp. 249-263, 2003. https://doi.org/10.1081/DRT-120017746
[13] S. von Graberg, *Freeze drying from small containers: Heat and mass transfer and implications on process design*. Erlangen, Germany: Friedrich-Alexander-Universität Erlangen-Nürnberg, 2011.
[14] N. P. Varma, "Computational fluid dynamics analysis of freeze drying process and equipment," Master's Thesis. Purdue University, West Lafayette, IN, USA, 2014.
[15] I. C. Trelea, S. Passot, M. Marin, and F. Fonseca, "Model for heat and mass transfer in freeze-drying of pellets," *arXiv preprint, hal-01536947*, 2009. https://doi.org/10.1115/1.3142975
[16] B. Scutellà, I. C. Trelea, E. Bourlés, F. Fonseca, and S. Passot, "Use of a multi-vial mathematical model to design freeze-drying cycles for pharmaceuticals at known risk of failure," in *Proceedings of the 21th International Drying Symposium, Valencia, Spain*, 2018, pp. 18-21.
[17] L. Gustafsson, "Determination of mass-and heat transfer coefficients for computer modelling of pharmaceutical freeze-drying," M.S. Thesis, Department of Food Technology, Engineering and Nutrition, Lund University, Lund, Sweden), 2021.
[18] T. Tongmai, M. Maketon, and P. Chumnanpuen, "Prevention potential of Cordyceps militaris aqueous extract against cyclophosphamind-induced mutagenicity and sperm abnormality in rats," *Agriculture and Natural Resources*, vol. 52, no. 5, pp. 419-423, 2018. https://doi.org/10.1016/j.anres.2018.11.005
[19] X. Liu, K. Huang, and J. Zhou, "Composition and antitumor activity of the mycelia and fruiting bodies of Cordyceps militaris," *Journal of Food and Nutrition Research*, vol. 2, no. 2, pp. 74-79, 2014.
[20] T. D. M. Carvalho, "Consistent scale-up of the freeze-drying process," Master's Thesis. Technical University of Denmark (DTU), Kongens Lyngby, Denmark, 2018.
[21] P. Munzenmayer *et al.*, "Freeze-drying of blueberries: Effects of carbon dioxide (CO2) laser perforation as skin pretreatment to improve mass transfer, primary drying time, and quality," *Foods*, vol. 9, no. 2, p. 211, 2020. https://doi.org/10.3390/foods9020211
[22] P. Foerst, S. Gruber, M. Schulz, N. Vorhauer, and E. Tsotsas, "Characterization of lyophilization of frozen bulky solids," *Chemical Engineering & Technology*, vol. 43, no. 5, pp. 789-796, 2020. https://doi.org/10.1002/ceat.201900500
[23] S. Gruber *et al.*, "Estimation of the local sublimation front velocities from neutron radiography and tomography of particulate matter," *Chemical engineering science*, vol. 211, p. 115268, 2020. https://doi.org/10.1016/j.ces.2019.115268
[24] T. L. Bergman, *Fundamentals of heat and mass transfer*, 8th ed. Hoboken, NJ: John Wiley & Sons, 2017.
[25] D. I. Onwude, N. Hashim, K. Abdan, R. Janius, and G. Chen, "Experimental studies and mathematical simulation of intermittent infrared and convective drying of sweet potato (Ipomoea batatas L.)," *Food and Bioproducts Processing*, vol. 110, pp. 1–42, 2018.
[26] M. Younis, D. Abdelkarim, and A. Zein El-Abedein, "Kinetics and mathematical modeling of infrared thin-layer drying of garlic slices," *Saudi Journal of Biological Sciences*, vol. 25, no. 2, pp. 232–238, 2017. https://doi.org/10.1016/j.sjbs.2017.06.011
[27] D. R. Heldman and D. B. Lund, *Handbook of food engineering*, 4th ed. Boca Raton, FL, USA: CRC Press, 2021.

Edelweiss Applied Science and Technology
ISSN: 2576-8484
Vol. 9, No. 6: 1905-1917, 2025
DOI: 10.55214/25768484.v9i6.8276

Appendix.
Symbols, significance and units

Symbol	Significance	Units	Symbol	Significance	Units
r	Radius	m	Q_u	Internal energy change	W
r_s	Radius of fiber	m	Q_{sub}	Heat for sublimation	W
r_{sub}	Radius of sublimation front	m	U_{dry}	Internal energy of the dry region	J
L_s	Length of fiber	m	D_{eff}	Mass diffusivity coefficient	m^2/s
A_{sub}	Sublimation area	m^2	J_w	Mass flux	$kg/m^2.s$
T_{conde}	Temperature of condenser	K	$\dot{G}$	Mass flux	kg/s
T_s	Temperature of surface fiber	K	$Y_{i,sim}$	Simulated values	
T_{froze}	Temperature of frozen region	K	$Y_{i,ex}$	Experimental values	
T_{sub}	Temperature of sublimation front	K	$Er_{(i)}$	Mean percentage error	
T_{shelf}	Temperature of shelf	K	τ	Time	s
T_{dry}	Temperature of the dried region	K	**Lower indices**		
P_{chamb}	Pressure at drying chamber	Pa	conde	Condenser	
P_w	Pressure saturation of vapor	Pa	cond,sub	Conduction heat: surface and sublimation front	
C_{dry}	Specific heat capacity	J/kg.K	cond,tr	Conduction heat: drying tray and fiber	
ρ_{dry}	Density of dyied region	kg/m^3	cont	Contact	
$\rho_{ice,eff}$	Density of ice	kg/m^3	dry	Dry region	
k_{dry}	Thermal conductivity of the dry region	W/m·K	eff	Effective	
c_w	Concentration of water	kg/m^3	ex	Experimental	
MR_0	Moisture content	kg/kgdb	froze	Frozen	
M_w	Molecular weight of water	kg/kmol	ice	Ice	
R_g	Gas constant	J/kmol.K	rad	Radiation	
L_{sub}	Latent heat of sublimation	J/kg	Rad,tr	Radiation heat: drying tray and fiber	
R_{cont}	Contact heat transfer resistance	K/W	s	Surface	
$R_{cond,sub}$	Conduct heat transfer resistance	K/W	sim	Simulation	
$R_{cond,tr}$	Conduct heat transfer resistance	K/W	shelf	Shelf plate	
R_{rad}	Radition heat transfer resistance	K/W	sub	Sublimation (front)	
$R_{rad,tr}$	Radition heat transfer resistance	K/W	tol	total	
Q_{rad}	Radiative heat transfer	W	w	water	
Q_{cont}	Contact heat transfer	W	0	Initial	

Edelweiss Applied Science and Technology
ISSN: 2576-8484
Vol. 9, No. 6: 1905-1917, 2025
DOI: 10.55214/25768484.v9i6.8276